Upregulation of ULK1 expression in PC-3 cells following tumor protein P53 transfection by sonoporation

YU WANG, YI-NI CHEN, WEI ZHANG, YU YANG, WEN-KUN BAI, E SHEN and BING HU

Department of Ultrasound in Medicine, Shanghai Jiao Tong University Affiliated Sixth People's Hospital, Shanghai Institute of Ultrasound in Medicine, Shanghai 200233, P.R. China

Received December 18, 2014; Accepted August 7, 2015

DOI: 10.3892/ol.2015.3946

Abstract. The aim of the present study was to investigate whether ultrasound combined with microbubbles was able to enhance liposome-mediated transfection of genes into human prostate cancer cells, and to examine the association between autophagy and tumor protein P53 (P53). An MTT assay was used to evaluate cell viability, while flow cytometry and fluorescence microscopy were used to measure gene transfection efficiency. Autophagy was observed using transmission electron microscopy. Reverse transcription-polymerase chain reaction (RT-PCR) and western blot analysis were used to assess the expression of autophagy-associated genes. The results of the present study revealed that cell viability was significantly reduced following successfully enhanced transfection of P53 by ultrasound combined with microbubbles. In addition, serine/threonine-protein kinase ULK1 levels were simultaneously upregulated. Castration-resistant prostate cancer is difficult to treat and is investigated in the present study. P53 has a significant role in a number of key biological functions, including DNA repair, apoptosis, cell cycle, autophagy, senescence and angiogenesis. Prior to the present study, to the best of our knowledge, increased transfection efficiency and reduced side effects have been difficult to achieve. Ultrasound is considered to be a 'gentle' technique that may be able to achieve increased transfection efficiency and reduced side effects. The results of the present study highlight a potential novel therapeutic strategy for the treatment of prostate cancer.

Introduction

Prostate cancer (PCa) is one of the leading causes of male urological cancer-associated mortality worldwide. Early stage PCa is androgen-dependent, and may be treated effectively using androgen ablation therapy, radiation and/or surgery. Although these treatments have largely been observed to be successful, there are associated disadvantages, including surgical injuries, drug resistance and tumor recurrence (1-3). In addition, all patients with PCa eventually progress to an androgen-independent state, known as castration-resistant prostate cancer (CRPC), which may lead to tumor metastasis or patient mortality (4). At present, there are no effective treatment options available for CRPC (5). Therefore, the development of novel therapeutic strategies is critical (6).

Gene therapy may be utilized to transfer normal target genes into abnormal cells, in order to achieve therapeutic benefits (7). At present, gene therapy is considered to be a novel method for the treatment of a number of diseases, and may represent a promising strategy for the treatment of cancer. In order to develop effective methods of gene transfer, numerous experimental and clinical studies have been undertaken (8). Tumor protein P53 (P53) has a critical role in a number of significant biological processes, including DNA repair, apoptosis, cell cycle, autophagy, senescence and angiogenesis (9). There are two types of P53: Wild-type (wt-P53), which promotes cell apoptosis, and mutant P53, which may enhance the growth of cancerous cells (10). Inactivation of the P53 system is associated with the onset and progression of cancer, and is a typical alteration characteristic of cancer cells: When this occurs, a P53-activating agent does not appear to work (11,12). A number of studies have also demonstrated that P53 is capable of stimulating autophagy (13-15).

ULK1 is part of a ULK1-complex, which contributes to various physiological and pathological processes in mammals and is an important protein in the early stages of autophagy (16). The upregulation of ULK1 allows for sustained autophagy and leads to an increase in non-apoptotic cell death. Notably, previous studies have indicated that ULK1 is a transcriptional target of p53 following DNA damage (17).

Previous studies have revealed that ultrasound, electric, laser and microinjection techniques may assist in the delivery of various therapeutic molecules, including genes and drugs (18-20). However, ultrasound is considered to be a 'gentle' technique. A number of studies have been undertaken to investigate how ultrasound may be capable of enhancing permeability of cells. The main mechanism is considered to be sonoporation. Sonoporation is similar to electroporation and

Correspondence to: Dr Bing Hu, Department of Ultrasound in Medicine, Shanghai Jiao Tong University Affiliated Sixth People's Hospital, Shanghai Institute of Ultrasound in Medicine, 600 Yishan Road, Shanghai 200233, P.R. China
E-mail: binghu1314@hotmail.com

Key words: autophagy, tumor protein P53, prostate cancer cell, sonoporation, ultrasound combined with microbubbles

refers to the generation of small pores in the cell membrane following irradiation by ultrasound and this has been revealed by high speed camera images (21); sonoporation is a non-invasive method that allows drugs or genes to enter cells (22,23). Sonoporation may result from oscillations of the microbubbles, which cause cavitation and subsequent disruption of membrane that allows to enhance permeability (24). These microbubbles, oscillating in the presence of US, create localized shear stress or 'microstreaming' or they may expand and collapse ('transient cavitation') to create intense local heating and pressure (25). This type of transient cavitation effect is considered to occur more at low frequencies (26). Previous research has suggested that the use of ultrasound combined with microbubbles may enhance the acoustic cavitation effect (27). However, further study is required in order to enhance transfection efficiency whilst simultaneously reducing harm to the body.

Materials and methods

Cell lines. The PC3 human prostate cancer cell line (The Cell Bank of the Chinese Academy of Sciences, Shanghai, China) was used in all experiments. Cells were incubated at 37˚C in an atmosphere of 5% CO_2. Dulbecco's modified Eagle's medium (DMEM) supplemented with 10% fetal bovine serum (FBS; Gibco, Life Technologies, Carlsbad, CA, USA) was used as culture medium and replaced every second day.

Ultrasound apparatus and microbubbles. The present experiment was performed using an FS-450 ultrasonic processor, supplied by the Shanghai Institute of Ultrasound in Medicine (Shanghai, China). In all experiments, the probe frequency was fixed at 21 kHz, the intensity was 4.6 mW/cm^2 and the duty cycle was 20% (2 sec 'on' time and 8 sec 'off' time) with a total exposure time of 5 min. The SonoVue™ microbubble echo-contrast agent (Bracco S.p.A, Milan, Italy) was reconstituted in 5 ml phosphate-buffered saline, 200 μl of which was used in each experimental group.

In the present study, cells were divided into three groups: A control group without treatment (Group A), a group treated with Lipofectamine® (Invitrogen Life Technologies, Carlsbad, CA, USA) and wt-P53/enhanced green fluorescent protein (EGFP) plasmid (Group B), and a group treated with Lipofectamine, wt-P53/EGFP plasmid and ultrasound combined with microbubbles (Group C). Experiments were performed in triplicate.

Preparation of plasmid DNA. The pEGFP plasmid (donated by the Center Laboratory of Shanghai Jiao Tong University Affiliated Sixth People's Hospital, Shanghai, China) DNA was used as a marker to indicate transfection efficiency and was prepared with the E.ZN.A Plasmid Miniprep kit II (Omega Bio-Tek, Inc., Norcross, GA, USA) in an identical manner to the wt-P53 plasmid DNA. The lysing solution from the Plasmid Miniprep kit was able to generate and lyse DH5α *Escherichia coli* transformants, which were of a density capable of expressing the target plasmid (28). The DNA-specific resin in a column was subsequently used to isolate plasmid DNA from genomic DNA, and the plasmid DNA was collected. The purity of the extracted pEGFP plasmid DNA was measured using an ultraviolet spectrophotometer (DU800; Beckman Coulter, Inc., Brea, CA, USA) whose optical density at 260/280 nm was 1.8. A digestive enzyme (*Sal*I or *Xho*I) and subsequent electrophoresis was used to identify pEGFP plasmid DNA (BD Biosciences, ClonTech, Palo Alto CA). Two restriction sites (*Sal*I and *Xho*I) were included to verify that the obtained plasmid was pEGFP when the genetic map was analyzed.

Table I. Oligonucleotide primer sequences for reverse transcription-polymerase chain reaction.

Gene	Primer sequence (5'-3')
ULK1	
Forward	AAGTTCGAGTTCTCTCGCAAG
Reverse	ACCTCCAGGTCGTGCTTCT
GAPDH	
Forward	AATGGATTTGGACGCATTGGT
Reverse	TTTGCACTGGTACGTGTTGAT

Gene transfer. Transfection experiments were performed according to the manufacturers's instructions. Transfection reagents were prepared according to the protocol of the Lipofectamine® 2000 kit (Invitrogen Life Technologies); the ratio of plasmid DNA (μg) to liposome (μl) was 1:2. Group A were the control cells, group B were the cells transfected with pEGFP/wt-P53 plasmid, and group C were the cells transfected with pEGFP/wt-P53 plasmid and treated with ultrsound combined with microbubble. Prior to ultrasound irradiation, the reagent was added to the suspension of PC3 cells in Group C. The density of the PC3 cells in polystyrene sample test tubes (Beijing Donglinchangsheng Biotechnology Co., Ltd., Beijing, China) was 1x10^5 cells/ml. Subsequently, the cell suspension was gently mixed with diluted plasmid DNA in 100 μl DMEM without FBS. Prior to use, Lipofectamine 2000 for Groups B and C was mixed gently and the appropriate amount was diluted in 100 μl DMEM without FBS. Following incubation for 5 min at room temperature, the diluted plasmid DNA (1 μg/100 μl) was combined with diluted Lipofectamine 2000 (2.5 μg/100 μl), mixed gently and incubated for 20 min at room temperature. Following 5 min of exposure to ultrasound with microbubbles, the cell suspensions were seeded into 6-well plates and 4 h later the serum-free DMEM was replaced by medium containing 10% FBS.

Detection of gene transfection efficiency. Following 24 h of incubation, pEGFP transfection efficiency was detected in the three groups using fluorescence microscopy and flow cytometry using a flow cytometer (Beckman Coulter, Fullerton, CA, USA). Images were captured using an A1RMP fluorescence microscope (Nikon Corporation, Tokyo, Japan). Cells were observed to express green fluorescence when successfully transfected with pEGFP DNA.

Measurement of cell proliferation by MTT assay. Following treatment, each group of cells was grown in 96-well plates for 24 h, and subsequently viability was assessed by MTT assay (Wellscan MK3; Ani Labsystems, Ltd., Oy, Vantaa, Finland). The assay was conducted as follows: 50 μl MTT

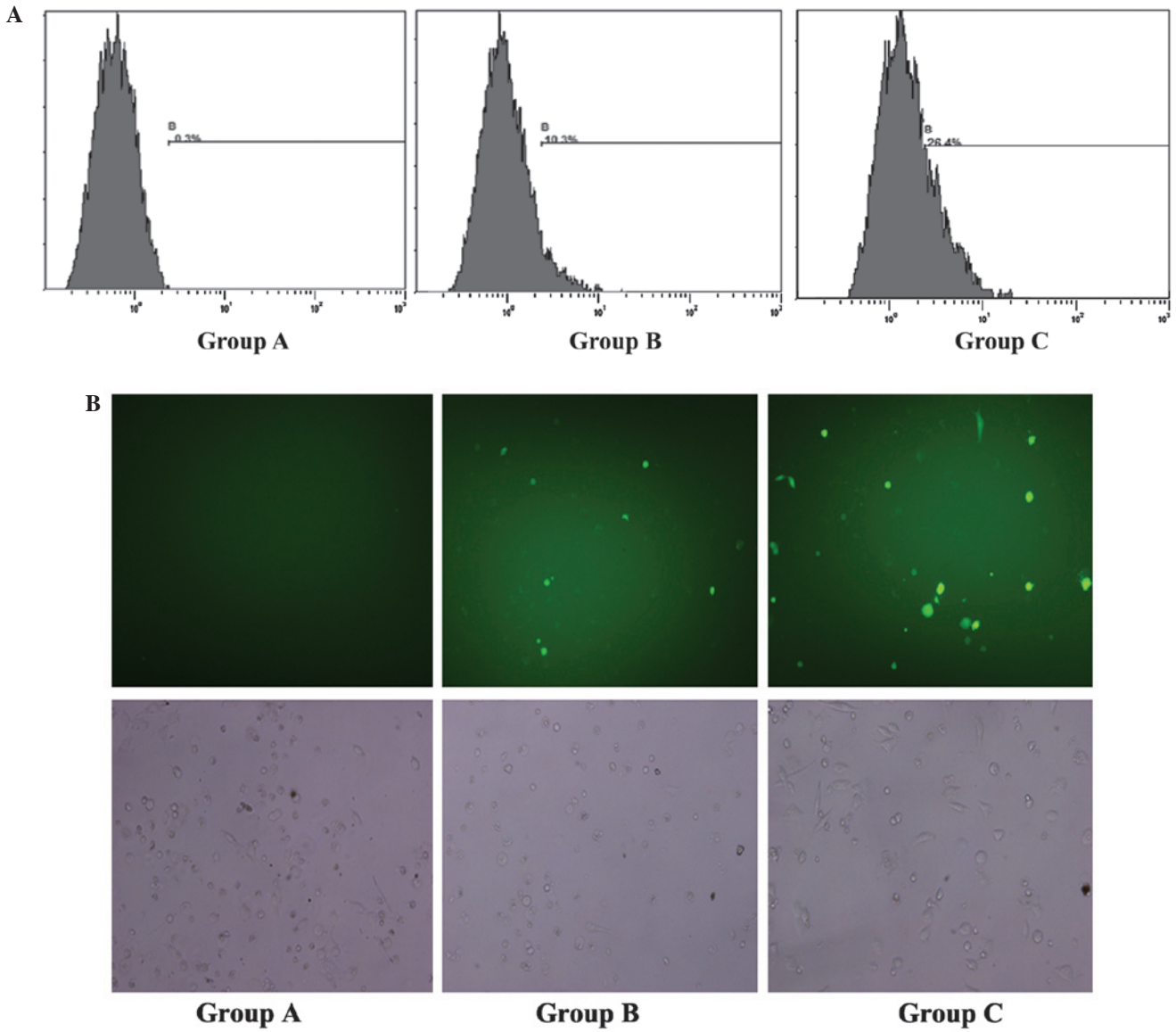

Figure 1. Gene transfection efficiency detected by flow cytometry and fluorescence microscopy. EGFP-positive rate of PC3 cells detected by (A) flow cytometry and (B) fluorescence microscopy (magnification, x200) 24 h following treatment in: Group A, no treatment; Group B, cells treated with Lipofectamine® and wt-P53/EGFP plasmid; and Group C, cells treated with Lipofectamine, wt-P53/EGFP plasmid and ultrasound combined with microbubbles. Top panel, green stain indicates successful transfection; bottom panel, brightfield view. EGFP, enhanced green fluorescent protein; P53, tumor protein P53; wt-P53, wild-type P53.

reagent was incubated with cells for 4 h at 37˚C and subsequently removed. Following this, 150 μl dimethyl sulfoxide was added to each well and agitated for 15 min. The optical density was measured at a wavelength of 492 nm using a BIO-TEK Synergy HT microculture plate reader (Bio-Tek Instruments, Inc., Winooski, VT, USA). The result was calculated as follows: Viability (%)=absorbance of experimental group/absorbance of control group x 100. Viability was calculated based on the mean percentage of triplicate experiments.

Transmission electron microscopy. PC3 cells from the three groups were sliced into ultra-thin specimens according to the conventional method (29). Specimens were then observed and images were captured using transmission electron microscopy (Hitachi S-4800; Hitachi, Ltd., Tokyo, Japan) at magnification, x24,500. Autophagosomes were identified by the characteristic structure of a double- or multi-lamellar smooth membrane completely surrounding compressed mitochondria, or membrane-bound electron-dense material. The investigator was blinded, and the numbers of autophagosomes in cells of each of the three groups were counted in 10 fields of view from various microscopic fields.

Reverse transcription-polymerase chain reaction (RT-PCR) analysis. Once grown to ~85% confluence, $5x10^6$ cells were harvested and the RNA was isolated using TRIzol reagent (Invitrogen Life Technologies) according to the manufacturer's instructions. The first strand of cDNA was generated from 2 mg total RNA using the SuperScript III Reverse Transcriptase kit (Invitrogen Life Technologies) according to the manufacturer's instructions. Following purification, RNA was subjected to PCR analysis on a Bio-Rad iQ5 multicolor detection system (Bio-Rad Laboratories, Inc., Hercules, CA, USA), using the following primers: ULK1, F 5'-TCGAGTTCT

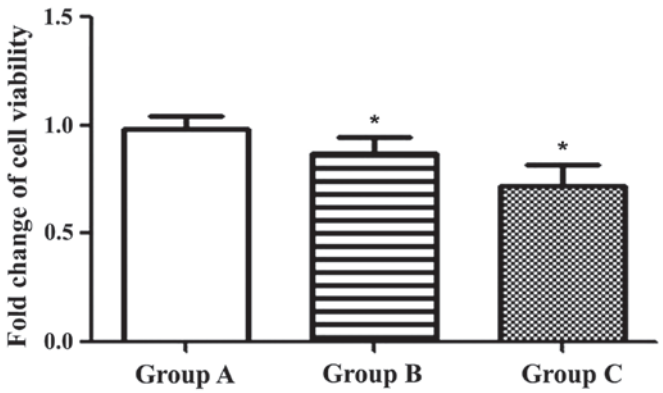

Figure 2. P53 transfection reduces cell viability. Group A, no treatment; Group B: cells treated with Lipofectamine® and wt-P53 plasmid; Group C: cells treated with Lipofectamine, wt-P53 plasmid and ultrasound combined with microbubbles. Values are expressed as the mean ± standard deviation. *P<0.05 vs. Group A. P53, tumor protein P53; wt-P53, wild-type P53.

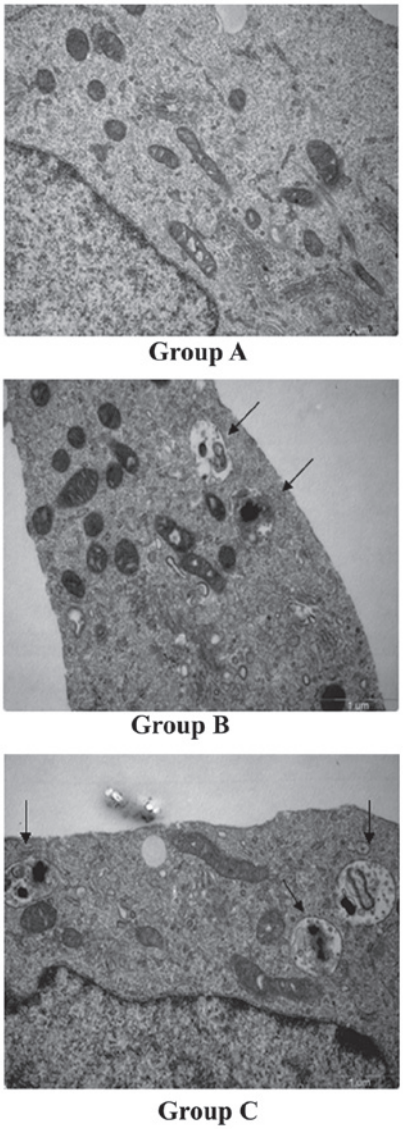

Figure 3. Autophagy is significantly increased in PC3 cells treated with ultrasound and microbubbles 24 h following treatment (magnification, x24,500). Group A, no treatment; Group B, cells treated with Lipofectamine® and wt-P53 plasmid; Group C: cells treated with Lipofectamine, wt-P53 plasmid and ultrasound combined with microbubbles. Arrows indicate autophagosomes. P53, tumor protein P53; wt-P53, wild-type P53.

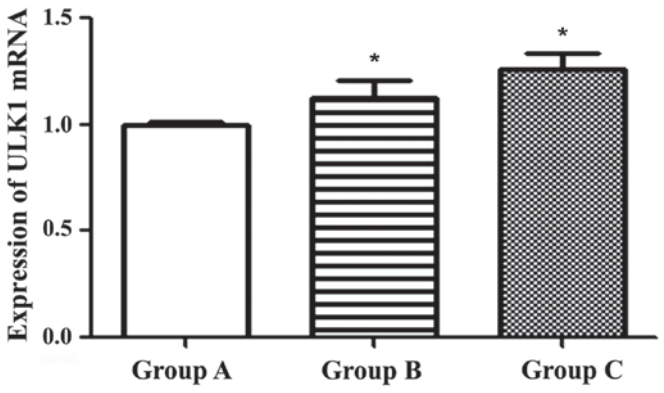

Figure 4. ULK1 mRNA expression is increased in Group C compared with Groups A and B following irradiation with ultrasound. Expression of ULK1 mRNA was examined using reverse transcription-polymerase chain reaction. Group A, no treatment; Group B, cells treated with Lipofectamine® and wt-P53 plasmid; Group C, cells treated with Lipofectamine, wt-P53 plasmid, and ultrasound combined with microbubbles. Values are expressed as the mean ± standard deviation. *P<0.05 vs. Group A. mRNA, messenger RNA; wt-P53, wild-type tumor protein 53.

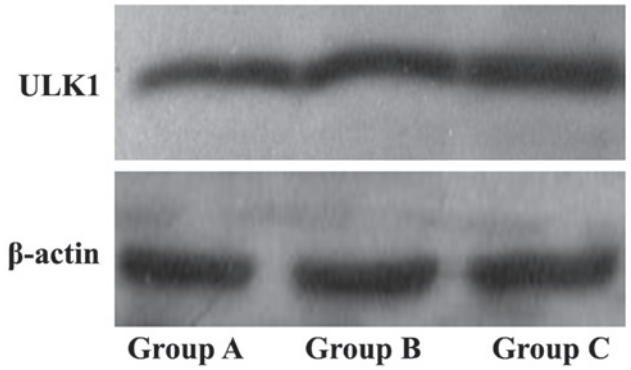

Figure 5. Expression of ULK1 protein is increased in PC3 cells of Group C following irradiation with ultrasound. Expression was examined using western blotting. Group A, no treatment; Group B, cells treated with Lipofectamine® and wt-P53 plasmid; Group C: cells treated with Lipofectamine, wt-p53 plasmid and ultrasound combined with microbubbles. wt-P53, wild-type tumor protein P53.

CCCGCAAGG-3' and CGTCTGAGACTTGGCGAGGT. The probe for ULK1 was CACCGCGAGAAGCACGATTTGGA. PCR was performed under the following conditions: 95˚C for 3 min followed by 40 cycles of 95˚C for 10 sec and 60˚C for 30 sec. GAPDH expression levels served as a control. The relative expression levels were calculated using the relative quantitative $2^{-\Delta\Delta Ct}$ method (30). The primer sequences used are indicated in Table I.

Western blot analysis. Cells were harvested using lysis buffer (radioimmunoprecipitation assay buffer), containing 20 mM Tris (pH 7.5), 150 mM sodium chloride, 1 mM EDTA, 1 mM ethylene glycol tetraacetic acid, 1% Triton X-100, 2.5 mM sodium pyrophosphate, 1 mM β-glycerophosphate, 1 mM sodium orthovanadate and protease inhibitors (10 μg/ml aprotinin, 1 μg/ml leupeptin and 0.1 mM phenylmethylsulfonyl fluoride) (Beyotime Institute of Biotechnology). Harvesting was performed when cells had grown to 80% confluence. Protein samples were collected, quantified

by SDS-PAGE (10-15%) and transferred onto a nitrocellulose membrane. The membranes were blocked using Tris-buffered saline containing 0.1% Tween-20 and 5% non-fat milk for 1 h. Protein samples were probed with rabbit polyclonal antibody specific for ULK1 (Santa Cruz Biotechnology, Santa Cruz, CA; 1:1,000) overnight at 4˚C and subsequently incubated with HRP-conjugated anti-rabbit IgG (Cell Signalling Technology, Boston, MA; 1:1,000) for 1 h at 25˚C. β-actin served as a control. Protein levels were visualized using an enhanced chemiluminescence system and band intensity was quantified using the SuperSignal chemiluminescent substrate (PerkinElmer, Inc., Waltham, MA, USA).

Statistical analysis. One-way analysis of variance was performed using SPSS version 13.0 software (SPSS Inc., Chicago, IL, USA). P<0.05 was considered to indicate a statistically significant difference. All experiments were performed at least in triplicate. Data are expressed as the mean ± standard deviation.

Results

Ultrasound treatment provides the most efficient transfection of P53. Gene transfection efficiency was detected using flow cytometry (Fig. 1A) and fluorescence microscopy (Fig. 1B). The results revealed that the wt-P53-EGFP-positive rate was highest in Group C (P<0.05). This suggested that the transfection efficiency of Group C was increased compared with that of Groups A and B. A significant difference in transfection efficiency was also observed between Groups A and B (P<0.05).

Transfection of P53 reduces cell viability. Following transfection, an MTT assay was used to evaluate cell viability. The results revealed that cell viability was 99.7±5.7% in Group A, 87.0±8.0% in Group B and 72.3±9.6% in Group C (Fig. 2). This demonstrated that wt-P53 was capable of inhibiting the growth of PC3 cells, and that ultrasound combined with microbubbles may enhance this effect.

Greater numbers of autophagosomes are present in Groups B and C. Autophagosomes have a characteristic structure of a double- or multi-lamellar membrane, which contains organelles or other decomposed residues (31). The numbers of autophagosomes in cells of each of the three groups were counted in 10 visions from various microscopic fields at a magnification of x24,500. Compared with Group A, the numbers of autophagosomes in Groups B and C were significantly increased (0.2±0.42 vs. 1.80 ±1.62 and 2.6±2.12; P<0.05; Fig. 3).

Serine/threonine-protein kinase ULK1 induces autophagy in PC3 cells. Levels of autophagy-associated gene ULK1 messenger RNA (mRNA) were significantly increased in Groups B and C, compared with Group A (Fig. 4). Levels of ULK1 mRNA were 1.00±0.02 in Group A, 1.13±0.08 in Group B and 1.26±0.08 in Group C (P<0.05).

Autophagy-related protein expression is enhanced in Groups B and C. Western blotting was used to assess autophagy-associated protein expression. ULK1 protein expression levels of the Groups B and C were observed to be increased compared with those of the control Group A (Fig. 5; P<0.05). Therefore, ultrasound combined with microbubble increased the expression levels of ULK1 protein.

Discussion

At present, ultrasound is not only widely used for the purpose of examination, but is also used as a treatment strategy, as it is non-invasive, safe and low cost (32). Microbubbles may be capable of enhancing the biological effects of ultrasound, by processes including increasing cell permeability, inhibiting tumor cell proliferation and inducing cell apoptosis (33). Cavitation is a significant effect of ultrasound. When microbubbles are irradiated by ultrasound, oscillation expansion, contraction and a series of other dynamic processes occur, leading to the 'cavitation effect'. Large shear forces and shock waves created by the cavitation effect generate holes in the membrane (34). This phenomenon is known as the 'sonoporation effect', and allows molecules outside the membrane to penetrate into the cells, and may subsequently improve the efficiency of delivery of therapeutic molecules into cells (35,36). Marmottant and Hilgenfeldt (37) suggest that low intensity ultrasonic irradiation, which induces vacuole vibration and microsound flow, may have the potential to alter cell membrane permeability. Prentice *et al* (38) hypothesized that irreversible sound perforation effects may be used in the treatment of cancer.

Three prostate cancer cell lines are known to possess varying P53 statuses: LNCaP is wild-type for P53, PC3 is null for P53 and DU145 is mutant-type for P53. PC3 cells were selected for use in the present study due to this absence of P53. Transfection assays of wt-P53-GFP plasmid were designed in order to detect whether ultrasound combined with microbubbles was able to enhance transfection. The flow cytometry and fluorescence microscopy results of the present study indicated that ultrasound combined with microbubbles was able to enhance transfection efficiency. An MTT assay was performed to detect whether this transfection induced cytotoxic effects and reduced the proliferation of tumor cells. Twenty-four hours following transfection, the cytotoxic effect of wt-P53 was found to be enhanced by ultrasound irradiation combined with microbubbles, due to enhanced rates of transfection and increased levels of wt-P53 in PC3 cells.

As a well-known tumor suppressor gene, wt-P53 may repair damaged genes in tumor cells and has been revealed to have a significant role in the prevention of cancer onset and progression (39). In addition, wt-P53 has a key role in the regulation of autophagosome formation (40). In the present study it was observed that, following successful transfection, P53-induced autophagy occurred. Results from transmission electron microscopy also suggested that autophagosome numbers were increased in Groups B and C, compared with those of Group A. Subsequently, western blot analysis and RT-PCR were performed to investigate ULK1 expression. ULK1 is a downstream target gene of wt-P53. When DNA is damaged, wt-P53 is able to adjust ULKI expression levels. Raised levels of the ULK1/Atg13 complex induced by wt-P53 are essential in order for autophagy to take place (17). To a certain extent, enhanced autophagy levels may promote cell apoptosis. In mammalian cells, ULK1-induced autophagy may inhibit certain types of cancer and increase the efficiency

of toxic chemotherapy drugs (17). In the present study, it was observed that ULK1 levels were upregulated in Groups B and C, and were highest in Group C. This confirmed that ultrasound combined with microbubbles was able to enhance the efficiency of the P53 gene, whose expression was not altered.

A number of studies have revealed that ultrasound combined with microbubbles is able to increase the efficacy of various types of therapeutic agents *in vivo* and that it is safe for normal tissues to be exposed to therapeutic techniques involving ultrasound. The present study represents an initial step towards the development of combination therapy for PCa. Further research may be required in order to gain an increased understanding of the underlying mechanisms of this technique and further development is required for these therapies to be translated into a clinical setting.

Acknowledgments

The present study was supported by the major infrastructure projects of Shanghai Science and Technology (grant no. 10JC1412600) and by the National Natural Science Foundation of China (grant nos. 81271597 and 81401421).

References

1. Tanaka G, Hirata Y, Goldenberg SL, Bruchovsky N and Aihara K: Mathematical modelling of prostate cancer growth and its application to hormone therapy. Philos Transact A Math Phys Eng Sci 368: 5029-5044, 2010.
2. Lecornet E, Ahmed HU, Moore C and Emberton M: Focal therapy for prostate cancer: A potential strategy to address the problem of overtreatment. Arch Esp Urol 63: 845-852, 2010.
3. Baumert H: Salvage treatments for prostatic radiation failure. Cancer Radiother 14: 442-445, 2010 (In French).
4. Chaturvedi S and Garcia JA: Novel agents in the management of castration resistant prostate cancer. J Carcinog 13: 5, 2014.
5. Shin SW, Kim SY and Park JW: Autophagy inhibition enhances ursolic acid-induced apoptosis in PC3 cells. Biochim Biophys Acta 1823: 451-457, 2012.
6. Jácome-Pita F, Sánchez-Salas R, Barret E, Amaruch N, Gonzalez-Enguita C and Cathelineau X: Focal therapy in prostate cancer: The current situation. Ecancermedicalscience 8: 435, 2014.
7. Wang W, Li W, Ma N and Steinhoff G: Non-viral gene delivery methods. Curr Pharm Biotechnol 14: 46-60, 2013.
8. Podolska K, Stachurska A, Hajdukiewicz K and Małecki M: Gene therapy prospects - intranasal delivery of therapeutic genes. Adv Clin Exp Med 1: 525-534, 2012.
9. Tasdemir E, Maiuri MC, Orhon I, Kepp O, Morselli E, Criollo A and Kroemer G: p53 represses autophagy in a cell cycle-dependent fashion. Cell Cycle 7: 3006-3011, 2008.
10. Rozan LM and El-Deiry WS: p53 downstream target genes and tumor suppression: A classical view in evolution. Cell Death Differ 14: 3-9, 2007.
11. Vogelstein B, Lane D and Levine AJ: Surfing the p53 network. Nature 408: 307-310, 2000.
12. Vousden KH and Lane DP: p53 in health and disease. Nat Rev Mol Cell Biol 8: 275-283, 2007.
13. Amaravadi RK, Yu D, Lum JJ, Bui T, Christophorou MA, Evan GI, Thomas-Tikhonenko A and Thompson CB: Autophagy inhibition enhances therapy-induced apoptosis in a Myc-induced model of lymphoma. J Clin Invest 117: 326-336, 2007.
14. Crighton D, Wilkinson S, O'Prey J, Syed N, Smith P, Harrison PR, Gasco M, Garrone O, Crook T and Ryan KM: DRAM, a p53-induced modulator of autophagy, is critical for apoptosis. Cell 126: 121-134, 2006.
15. Feng Z, Hu W, de Stanchina E, Teresky AK, Jin S, Lowe S and Levine AJ: The regulation of AMPK beta1, TSC2, and PTEN expression by p53: Stress, cell and tissue specificity, and the role of these gene products in modulating the IGF-1-AKT-mTOR pathways. Cancer Res 67: 3043-3053, 2007.
16. Mizushima N: The role of the Atg1/ULK1 complex in autophagy regulation. Curr Opin Cell Biol 22: 132-139, 2010.
17. Gao W, Shen Z, Shang L and Wang X: Upregulation of human autophagy-initiation kinase ULK1 by tumor suppressor p53 contributes to DNA-damage-induced cell death. Cell Death Differ 18: 1598-1607, 2011.
18. Deng CX, Sieling F, Pan H and Cui J:Ultrasound-induced cell membrane porosity. Ultrasound Med Biol 30: 519-522, 2004.
19. Lawrie A, Brisken AF, Francis SE, Cumberland DC, Crossman DC and Newman CM: Microbubble-enhanced ultrasound for vascular gene delivery. Gene Ther 7: 2023-2024, 2000.
20. Kim HJ, Greenleaf JF, Kinnick RR, Bronk JT and Bolander ME: Ultrasound-mediated transfection of mammalian cells. Hum Gene Ther 7: 1339-1346, 1996.
21. Xu Z, Raghavan M, Hall TL, Chang CW, Mycek MA, Fowlkes JB and Cain CA: High speed imaging of bubble clouds generated in pulsed ultrasound cavitational therapy - histotripsy. IEEE Trans Ultrason Ferroelectr Freq Control 54: 2091-2101, 2007.
22. Tachibana K and Tachibana S: Transdermal delivery of insulin by ultrasonic vibration. J Pharm Pharmacol 43: 270-271, 1991.
23. Wang W, Li W, Ma N and Steinhoff G: Non-viral gene delivery methods. Curr Pharm Biotechnol 14: 46-60, 2013.
24. Husseini GA and Pitt WG: The use of ultrasound and micelles in cancer treatment, J Nanosci Nanotechnol 8: 2205-2215, 2008.
25. Juffermans LJ, van Dijk A, Jongenelen CA, Drukarch B, Reijerkerk A, de Vries HE, Kamp O and Musters RJ: Ultrasound and microbubble-induced intra- and intercellular bioeffects in primary endothelial cells, Ultrasound Med Biol 35: 1917-1927, 2009.
26. Hoskins P, Thrush A, Martin K and Whittingam T (eds): Diagnostic Ultrasound: Physics and Equipment. 2nd Edition. Cambridge University Press, New York, NY, 2010.
27. Nyborg WL: Acoustic streaming. In: Nonlinear Acoustics. Hamilton NF and Blackstock DT (eds). Blackstock Academic Press, San Diego, pp207-232, 1998.
28. Wooley RE1, Gibbs PS, Dickerson HW, Brown J and Nolan LK: Analysis of plasmids cloned from a virulent avian Escherichia coli and transformed into Escherichia coli DH5 alpha. Avian Dis 40: 533-539, 1996.
29. Hinescu ME, Gherghiceanu M, Suciu L and Popescu LM: Telocytes in pleura: Two- and three-dimensional imaging by transmission electron microscopy. Cell Tissue Res 343: 389-397, 2011.
30. Lu Y1, Chen X, Wu Y, Wang Y, He Y and Wu Y: Directly transforming PCR-amplified DNA fragments into plant cells is a versatile system that facilitates the transient expression assay. PLoS One 8: e57171, 2013.
31. Eng KE, Panas MD, Murphy D, Karlsson Hedestam GB and McInerney GM: Accumulation of autophagosomes in Semliki Forest virus-infected cells is dependent on expression of the viral glycoproteins. J Virol 86: 5674-5685, 2012.
32. Zheng X, Ji P and Hu J: Sonoporation using microbubbles promotes lipofectamine-mediated siRNA transduction to rat retina. Bosn J Basic Med Sci 11: 147-152, 2011.
33. Tsunoda S,Mazda O, Oda Y, Iida Y, Akabame S, Kishida T, Shin-Ya M, Asada H, Gojo S, Imanishi J, *et al*: Sonoporation using microbubble BR14 promotes pDNA/siRNA transduction to murine heart. Biochem Biophys Res Commun 336: 118-127, 2005.
34. Geers B, Lentacker I, Alonso A, Sanders NN, Demeester J, Meairs S and De Smedt SC: Elucidating the mechanisms behind sonoporation with adeno-associated virus-loaded microbubbles. Mol Pharm 8: 2244-2251, 2011.
35. Nomikou N and McHale AP: Exploiting ultrasound-mediated effects in delivering targeted, site-specific cancer therapy. Cancer Lett 296: 133-143, 2010.
36. Richardson ES, Pitt WG and Woodbury DJ: The role of cavitation in liposome formation. Biophys J 93: 4100-4107, 2007.
37. Marmottant P and Hilgenfeldt S: Controlled vesicle deformation and lysis by single oscillating bubbles. Nature 423: 153-156, 2003.
38. Prentice PA, McLean D, Cuschieri A, Dholakia K and Campbell PA: Spatially controlled sonoporation of prostate cancer cells via ultrasound activated microbubble cavitation. In: 3rd IEEE/EMBS Special Topic Conference on Microtechnology in Medicine and Biology. IEEE, New York, pp158-159, 2005.
39. Xu J, Singh A and Amiji MM: Redox-responsive targeted gelatin nanoparticles for delivery of combination wt-p53 expressing plasmid DNA and gemcitabine in the treatment of pancreatic cancer. BMC Cancer 14: 75, 2014.
40. Green DR and Kroemer G: Cytoplasmic functions of the tumor suppressor p53. Nature 458: 1127-1130, 2009.